Universality in disordered diffusive systems: Exact fixed points in one, two, and three dimensions

P. B. Visscher
Department of Physics and Astronomy, University of Alabama, University, Alabama 35486
(Received 24 June 1983)

We analyze the behavior of discrete-time equations of motion for two-component diffusive systems under renormalization transformations, near a fixed point. We calculate the largest eigenvalues and their eigenfunctions exactly, thus determining the universal large-scale behavior of such a system. The special case in which the diffusivity of one component (the "scatterers") vanishes is equivalent to the problem of diffusion of the other component (the "electrons") in the presence of static disorder. Specific models of this type have been previously studied and are known to have anomalous long-time behavior: In one dimension, the mean-square displacement has a nonanalytic term proportional to $t^{1/2}$. We verify the universality of this behavior, and determine the universal nonanalytic behavior in two dimensions (a logarithmic term) and in three dimensions ($t^{-1/2}$). The amplitudes of the terms are obtained exactly for the most common model.

I. INTRODUCTION

Considerable interest has recently been focused on the problem of diffusion in disordered systems.[1] It appears that theoretical understanding of such systems is useful in explaining certain experimental phenomena, such as impurity conduction in semiconductors,[2,3] hopping conduction in amorphous semiconductors,[4,5] and low-frequency conductivity in superionic conductors.[6] Theoretical study of disordered systems has been most successful in one dimension, in which the long-time (low-frequency) behavior is known to be nonanalytic:[7–9] the mean-square displacement $\langle r^2(t)\rangle$ has a $t^{1/2}$ term as well as the usual diffusion term proportional to t.

The purpose of the present paper is to apply techniques developed for renormalization-group analysis of discrete equations of motion to this problem.[10] A system in which electrons diffuse through static disorder can be regarded as the $D^s\to 0$ limit of a two-component diffusive system in which electrons and scatterers both diffuse, with diffusivities D^e and D^s. We will analyze this system for arbitrary D^s. We will show that not only can the known one-dimensional behavior be straightforwardly obtained by our discrete method, but the method applies equally well to higher dimensionality, in which only approximate calculations have previously been done.

In Sec. II we will briefly review the method of discrete hydrodynamics and the precise definitions of time- and space-coarsening transformations introduced in the preceding paper;[10] it is intended that the present paper be self-contained. In Sec. III we construct an invariant manifold of equations of motion for two-component systems containing the fixed points as well as the scattering perturbations of interest. These are used in Sec. IV to compute exactly the largest eigenvalues and their eigenfunctions for the coarsening transformation linearized around the fixed point. From these we obtain, in Sec. V, the universal long-time behavior of such interacting systems, and then display the universal behavior of the mean-square displacement in Sec. VI ($d=1$) and Sec. VII ($d=2$ and 3). It is emphasized that this approach is not limited to the calculation of asymptotic power laws whose amplitudes must be fit to the properties of specific systems; we compute some exact amplitudes for specific models. For any microscopic model, amplitudes can be calculated by carrying out the coarsening transformations numerically.[11] This determines the behavior on any larger scale than the microscopic one, in a way which is guaranteed to give the correct universal long-time limit.

II. DISCRETE EQUATIONS OF MOTION AND COARSENING TRANSFORMATIONS

We will use the discrete equations of motion described for a one-component system in Ref. 10. Briefly, these describe a system on a length scale Δr and a time scale Δt, through cell contents c_p; the subscript p indicates that this is a physical (not dimensionless) content. We generalize to a two-component system by adding a superscript $\alpha=e$ (electron) or s (scatterer). Thus $c_p^e(r_p,t_p)$ is the mass of electrons in a cubical cell (Δr on a side) centered at position r_p, at time t_p (a multiple of Δt), and $c_p^s(r_p,t_p)$ is the mass of scatterers. For purposes of scale coarsening, we construct an equation of motion (EOM) in terms of dimensionless contents

$$c^\alpha(r,t)=c_p^\alpha(r\,\Delta r,t\,\Delta t)/\Delta c^\alpha\ , \tag{2.1}$$

where r is the dimensionless position vector of the center of a cell of size 1, the integer t is a dimensionless time, and Δc^e and Δc^s are conveniently chosen mass units for electrons and scatterers, respectively. The system can be described by equilibrium time correlation functions of the c's, or alternatively by a set of "equation-of-motion coefficients." These describe the probability distribution of the contents $c^\alpha(r,1)$ at time Δt in an ensemble having fixed contents $c(r,0)$ at time $t=0$. A moment in this ensemble is distinguished by square brackets [ ], and expanded as a power series in the $c(r,0)$'s,

$$[c^{\alpha}(r,1)]=\sum_{r',\alpha'}[c^{\alpha}(r,1)]_{c^{\alpha'}(r',0)}c^{\alpha'}(r',0)+\sum_{r',\alpha'}\sum_{r'',\alpha''}[c^{\alpha}(r,1)]_{c^{\alpha'}(r',0)c^{\alpha''}(r'',0)}c^{\alpha'}(r',0)c^{\alpha''}(r'',0)+\cdots . \tag{2.2}$$

The square brackets with c^{α}'s as subscripts are just constants, the coefficients in the power series. There is no constant term in Eq. (2.2) because we have redefined c^{α} by subtracting the equilibrium average $\langle c^{\alpha}\rangle$; it follows that $[c^{\alpha}(r,1)]=0$ when $c^{\alpha}(r,0)=0$.

The corresponding equation for the second moment does have a constant term, for which we use a subscript 1 (formally, the product of zero c^{α}'s),

$$[c^{\alpha}(r,1)c^{\alpha'}(r',1)]=[c^{\alpha}(r,1)c^{\alpha'}(r',1)]_1+\cdots . \tag{2.3}$$

The term $[cc]_1$ describes the conditional fluctuations of the contents. We can also define moments in ensembles in which $m>1$ earlier contents are constrained: In the mth ensemble, $c^{\alpha}(\ldots,0)$, $c^{\alpha}(\ldots,-1)$, and $c^{\alpha}(\ldots,1-m)$ are constrained. The power-series coefficients in these variables (describing non-Markovian behavior) are necessary in order to describe the system completely.[10,12] In the present paper, however, we will deal mostly with the continuous-space limit[10] in which the non-Markovian effects are negligible, and the coefficients in Eqs. (2.2) and (2.3) (having $m=1$) uniquely specify the system. In particular, we will show later that they determine the equilibrium equal-time correlations among the contents, which we denote by angular brackets: $\langle c^{\alpha}(r,t)c^{\alpha'}(r',t')\rangle$.

The coefficients in Eq. (2.2) will be sometimes referred to as "propagators." A general propagator may be denoted $[c^{\alpha}(r,1)c^{\alpha'}(r',1)\cdots]_{c^{\tilde{\alpha}}(r,0)\cdots}$. It is a function only of the differences between the r's, and can be most conveniently treated in terms of its Fourier transform,[10] denoted $G^{\alpha\alpha'\cdots}_{\tilde{\alpha}\tilde{\alpha}'\cdots}$. For example,

$$(2\pi)^d\delta_{2\pi}(k-k')G^{\alpha}_{\alpha'}(k,1;k',0)=\sum_{r,r'}e^{-ikr+ik'r'}[c^{\alpha}(r,1)]_{c^{\alpha'}(r',0)} \tag{2.4}$$

defines $G^{\alpha}_{\alpha'}$. This is a special case of a general formula given in Ref. 10 [Eq. (4.1)]. Here $\delta_{2\pi}$ is a Dirac δ function with period 2π in each of the d spatial dimensions which is factored out to make G nonsingular; G itself need not be defined except at $k=k'$. This propagator describes the effect of the cell content of component α' at $t=0$ on the content of component α at $t=1$.

The Fourier transform (FT) of the conditional fluctuation coefficient $[cc]_1$ in Eq. (2.3) is a "fluctuation propagator" $G^{\alpha\alpha'}$,

$$(2\pi)^d\delta_{2\pi}(k+k')G^{\alpha\alpha'}(k,1,k',1)=\sum_{r,r'}e^{-ikr-ik'r'}[c^{\alpha}(r,1)c^{\alpha'}(r',1)] . \tag{2.5}$$

We will also consider the FT of the corresponding equilibrium average, which we will denote by $G^{\alpha\alpha'}_{\rm eq}$.

We will also deal with the nonlinear propagator

$$(2\pi)^d\delta_{2\pi}(k-k'-k'')G^{\alpha}_{\alpha'\alpha''}(k,1;k',0,k'',0)=\sum_{r,r',r''}e^{ikr-ik'r'-ik''r''}[c^{\alpha}(r,1)]_{c^{\alpha'}(r',0)c^{\alpha''}(r'',0)} , \tag{2.6}$$

which describes the effect of components α' and α'' on component α; the special case G^{e}_{es} will be used in Sec. V to describe the effects of scatterers (component label $\alpha=s$) on electrons ($\alpha=e$).

Note that the time arguments in Eqs. (2.4)—(2.6) are redundant, as is one of the wave vectors (because of translational invariance.) We will usually omit the redundant arguments, writing, for example, $G^{\alpha}_{\alpha'}(k)$ in Eq. (2.4).

We will regard an equation of motion E as being specified by the totality of these propagators G [Eqs. (2.4)—(2.6)]. (This differs from the viewpoint of Ref. 10, in which the equilibrium fluctuation $G^{\alpha\alpha'}_{\rm eq}$ was used instead of the fluctuation propagator $G^{\alpha\alpha'}$.)

We will want to perform space- and time-coarsening transformations S and T, and mass-rescaling transformations R_{α}, on an equation of motion E which describes a system on the scale Δr, Δt, Δc^{e}, and Δc^{s}. We define S, T, and R_{α} by requiring that SE describe the same system on the scale $2\Delta r$, Δt, Δc^{e}, and Δc^{s}, that TE describe it on the scale in which $2\Delta t$ replaces Δt, and that $R_{\alpha}E$ describe it when $2\Delta c^{\alpha}$ replaces Δc^{α}. The action of the R_{α}'s on the propagators is straightforward, and was described for the one-component case in Ref. 10. In general, R_{α} divides G by a factor of 2 for each predicted c^{α} factor, and multiplies G by a factor of 2 for each such constrained content. Thus if E is described by $G^{s}_{s},G^{e}_{s},G^{ss},\ldots$, the rescaled $E'=R_sE$ is described by

$$[G^{s}_{s}(k)]'=G^{s}_{s}(k) , \tag{2.7a}$$

$$[G^{e}_{s}(k)]'=2G^{e}_{s}(k) , \tag{2.7b}$$

$$[G^{ss}(k)]'=2^{-2}G^{ss}(k) . \tag{2.7c}$$

(The square bracket no longer denotes an average in a special ensemble: the G's are just functions.)

Space coarsening was also considered in detail in Ref. 10, and the results can be generalized to the two-component case. In the continuous-space limit, S involves just rescaling the distance variables. In terms of the Fourier transform, each equilibrium average has[10] a factor of 2^d and each k is replaced by $k/2$. For example,

$$[G^{\alpha\alpha'}_{\rm eq}(k)]'=2^dG^{\alpha\alpha'}_{\rm eq}(k/2) . \tag{2.8}$$

One can show from the equations (Appendix C) relating these equilibrium averages to the propagators defined in smaller ensembles that there is one fewer factor of 2^d for each constrained variable. That is,

$$[G^{\alpha\alpha'\cdots}_{\tilde{\alpha}\tilde{\alpha}'\cdots}(k,\ldots)]'=2^{d(1-n_c)}G^{\alpha\alpha'\cdots}_{\tilde{\alpha}\tilde{\alpha}'\cdots}(k/2,\ldots) , \tag{2.9}$$

where n_c is the number of constrained-variable indices $\tilde{\alpha},\tilde{\alpha}',\ldots$. In particular,

$$[G^{\alpha}_{\alpha'}(k)]'=G^{\alpha}_{\alpha'}(k/2) . \tag{2.10}$$

The case of time coarsening is less simple. Basically it involves combining the propagators that go from $t=0$ to 1 with those that go from $t=1$ to 2 to obtain a propagator describing evolution from $t=0$ to 2. General methods for calculating these time-coarsened propagators in real space are described in Appendix A and in k space in Appendix D. These involve associating an "EOM graph" with each

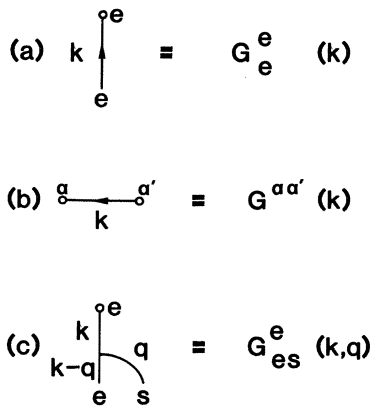

FIG. 1. Graphical representation of propagators. The vertical coordinate is time; the top of each graph is $t=1$. There is one external vertex for each predicted or constrained content [the internal intersection in (c) is not considered a vertex]; those corresponding to predicted variables are decorated with circles. Each is labeled by the corresponding component label α (equal to e or s). The corresponding k vector is written by the line leading to the vertex. Because of k-vector conservation (translational invariance) there are one fewer independent k's than vertices. When it is unclear [e.g., in (a) and (b)] which vertex k refers to, an arrow is drawn (toward it if predicted, away if not); the other vertex has $-k$.

EOM coefficient G, as indicated in Fig. 1. Here we will describe the time-coarsening of the electron propagator G_e^e from a graphical point of view. The time-coarsened $G_e^{e\prime}$ has the two terms shown in Fig. 2. Our previous one-component result,[10]

$$[G_e^e(k)]'=G_e^e(k)G_e^e(k)\ , \tag{2.11}$$

is represented graphically (using the rules at the end of Appendix D) by the first term in Fig. 2: An electron "propagates" from $t=0$ to 1 to 2 ($t=2$ means $t'=1$ in terms of the coarse time scale). The second term allows for the possibility (if physically allowed) that it will turn into an s between $t=0$ and 1, and then turn back into an e.

III. INVARIANT MANIFOLD FOR A TWO-COMPONENT SYSTEM

In Ref. 10 we were able to analyze the universal large-scale behavior of one-component diffusive systems by identifying a family of EOM's which are fixed points of a combination $ST^2R^{d/2}$ of the transformations S, T, and R. We will obtain these fixed points here as a special case of a much more general manifold of EOM's. The family

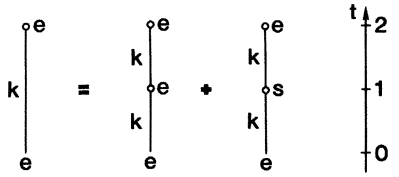

FIG. 2. Diagrams for time-coarsening the electron propagator in a two-component system [Eq. (2.11)].

of fixed EOM's is parametrized by the diffusivity D and the mean-square content fluctuation A. It is easiest to describe in the continuous-space limit ($\Delta r\to 0$ for fixed physical diffusivity so the dimensionless D becomes large), and this limit is sufficient because the general case can be calculated from it [see Eq. (3.20)]. In this limit, the fixed point has the one-particle propagator

$$G_\alpha^\alpha(k)=\exp(-Dk^2)\ , \tag{3.1}$$

and the equilibrium equal-time fluctuations

$$G_{\rm eq}^{\alpha\alpha}(k)=A\ . \tag{3.2}$$

In Ref. 10 we generalized these propagators to a broader family of EOM's parametrized by additional parameters such as the Burnett coefficients, within which we could carry out an eigenvalue analysis of the coarsening transformation which determined the universal large-scale behavior. Here, we will describe a less straightforward but more elegant method of defining such a family of EOM's, which we will call an "invariant manifold" because it is closed under the coarsening transformations. Unlike the previous formulation, this method is generalizable to nonlinear and multicomponent systems.

First note that we can view the propagator in Eq. (3.1) as the exponential of a "generating propagator"

$$G_g(k)=-Dk^2\ . \tag{3.3}$$

It turns out that the entire EOM (including fluctuations) may be viewed similarly as the exponential of a "generating EOM," which includes a fluctuation propagator such as Eq. (2.5) (and will, in a two-component system, also involve nonlinear interaction propagators). To make sense of this, we must first define what is meant by the exponential of an EOM containing these various propagators. We define in Appendix B precisely what it means to multiply two EOM's, E_a and E_b; basically E_bE_a is the EOM which evolves a system forward in time by applying E_a and then E_b. If $E_a=E_b$, this amounts to time coarsening: $E_aE_a=TE_a$. For the simplest propagator $G_\alpha^\alpha(k)$ in a one-component system [which we may refer to as $G(k)$, since α takes on only one value], multiplication of EOM's simply involves multiplication of the propagators,

$$G(k)=G_a(k)G_b(k)\ . \tag{3.4}$$

The multiplicative identity is an EOM denoted 1_E whose only nonzero propagators are

$$G_\alpha^\alpha(k)=1\ . \tag{3.5}$$

Evidently, 1_E can be thought of as evolution through a time interval of zero length; the propagators leave the electrons and scatterers exactly where they were. We also need a notion of addition: Let us define each of the propagators of $E=E_a+E_b$ to be the sum of the corresponding propagators of E_a and E_b. Omitting the α sub- and superscripts, we can write this schematically as

$$G=G_a+G_b\ . \tag{3.6}$$

Given an identity and notions of multiplication and addition, we can, of course, define exponentiation by

$$\exp(E_g)=\lim_{n\to\infty}(1_E+E_g/n)^n . \tag{3.7}$$

It is then clear that for a one-component system this gives the correct fixed-point one-particle propagator [Eq. (3.1)] from the generator in Eq. (3.3): Exponentiation of the propagators reduces to exponentiation of real numbers because of the simple relation (3.4)

We would like to obtain the entire fixed-point EOM (including fluctuations) this way, that is, by including a fluctuation propagator in the generator. Let us consider the most general generator for the fluctuation propagator $G^{\alpha\alpha}(k)$ [Eq. (2.5)]. In a conservative system, it must vanish when $k=0$ (the total content cannot fluctuate), and symmetry requires it to be even in k. We will later write the general form [Eq. (3.13)], but the simplest such function clearly is a constant multiplied by k^2,

$$G^{\alpha\alpha}(k)=ak^2 . \tag{3.8}$$

Let us examine the fluctuations produced by exponentiating a generating EOM consisting of the fluctuation propagator [Eq (3.8)] and the diffusion propagator [Eq. (3.3)]. We will do this by a general perturbative procedure which can be used to expand any exponential e^{E+F} in powers of F, where E is an "unperturbed" generator (here it contains only the one-particle propagator [Eq. (3.3)]) and F is the perturbation [here Eq. (3.8), the fluctuation propagator]. The procedure is described in detail in Appendix E, and gives for the conditional fluctuation

$$G^{\alpha\alpha}(k)=\int_0^1 du\,\exp[-Dk^2(1-u)] \times\exp[-D(-k)^2(1-u)]ak^2 \tag{3.9a}$$

$$=\frac{a}{2D}[1-\exp(-2Dk^2)] . \tag{3.9b}$$

Equation (3.9a) is obtained from the graph in Fig. 3, and can be understood heuristically as follows: At time u the fluctuation generator $F=ak^2$ acts, creating two fluctuations with momenta k and $-k$. Each of these evolves from time u to time 1 according to the propagator $\exp[-D(\pm k)^2(1-u)]$ from the EOM $e^{E(1-u)}$. This accounts for all of the factors in Eq. (3.9a), which must be integrated with respect to the time u at which the perturbation F acts.

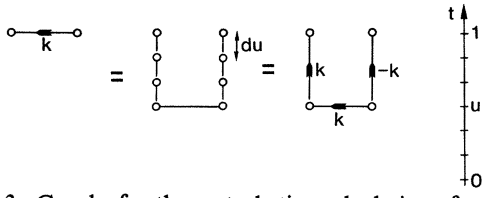

FIG. 3. Graphs for the perturbative calculation of one of the propagators [$G^{\alpha\alpha}(k)$, the left-hand graph] of the exponential e^{E+F}, where E has only the propagator $G^{\alpha}_{\alpha}(k)=-Dk^2$ and F has $G^{\alpha\alpha}(k)=ak^2$. Details are described in Appendix E. In the middle ("rosary") graph [which represents the right-hand side of Eq. (E2)] the short vertical lines are propagators from $1_E+E\,du$ (i.e., are $1-Dk^2du$) and the horizontal line is ak^2du from $F\,du$. In the right-hand ("topological") graph (which represents the sum of all rosary graphs with this topology, having F's at different times u) the vertical propagators are $G^{\alpha}_{\alpha}(k)=\exp(-Dk^2\Delta u)$ from the EOM $e^{E\Delta u}$, where $\Delta u=1-u$.

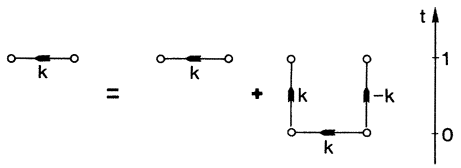

FIG. 4. Graphs for computing the equilibrium average $G^{\alpha\alpha}_{\rm eq}$ (left-hand side) from the fluctuation propagator $G^{\alpha\alpha}$ (first term on the right, an average in the ensemble in which contents at $t=0$ are constrained), according to the rules of Appendixes C and D. Those subgraphs on the right-hand side having no decorated vertices (circles) at $t=0$ refer to the constrained ensemble; the one with such decorations refers to the equilibrium ensemble.

We can check that the equilibrium fluctuations created by the fluctuation generator [Eq. (3.8)] via the fluctuation propagator [Eqs. (3.9)] are the ones [Eq. (3.2)] we expect at the fixed point for a one-component system. This can be done by a graphical procedure described in detail in Appendix C; it is a general method for computing EOM coefficients in a large ensemble from those in a smaller ensemble. The present problem is a special case in which the large ensemble is the equilibrium ensemble (in which the "EOM coefficients" are just equilibrium averages such as $G^{\alpha\alpha}_{\rm eq}$), and the small ensemble is the ensemble in which all variables at times $t\le 0$ are constrained and the corresponding EOM coefficient is $G^{\alpha\alpha}$. The graphical equation involved in this case is shown in Fig. 4. Using the rules in Appendix D to turn it into an equation for the Fourier transforms, we obtain

$$G^{\alpha\alpha}_{\rm eq}(k)=G^{\alpha\alpha}(k)+G^{\alpha}_{\alpha}(k)G^{\alpha}_{\alpha}(-k)G^{\alpha\alpha}_{\rm eq}(k) . \tag{3.10}$$

The product term represents the amount of the $t=0$ equilibrium fluctuation which remains after propagating to $t=1$ via G^{α}_{α}; adding the newly generated fluctuation $G^{\alpha\alpha}$ must recreate, at $t=1$, the equilibrium fluctuation. With use of Eq. (3.1) for G^{α}_{α}, the solution is Eq. (3.2), as promised. The mean-square fluctuation is given by

$$A=a/2D , \tag{3.11}$$

as one might have guessed by thinking of A as resulting from a dynamic equilibrium between the creation of fluctuations (at the rate a) and their decay (at the rate $2D$).

We have now shown that we can express the fixed-point EOM's in a simple exponential form [Eq. (3.7)], with generators given by Eqs. (3.3) and (3.8). These are now very easy to generalize, by replacing each propagator by a general power series in k. Equation (3.3) becomes

$$G^{\alpha}_{\alpha}(k)=D_0-D_2k^2-D_4k^4-\cdots , \tag{3.12}$$

where D_0 is a decay rate (zero in the present application, where we assume conservation of particles), D_2 is the diffusivity D, and D_4 is a Burnett coefficient.[10] The generalization of the fluctuation propagator [Eq. (3.8)] can be written

$$G^{\alpha\alpha}(k)=ak^2\exp(-\xi^2k^2-\lambda_4k^4-\cdots) . \tag{3.13}$$

We use this form rather than a simple power series so that

ξ will be interpretable as a correlation length; the k^0 term again vanishes in a conservative system. We now have a manifold of EOM's

$$E(D_0,D_2,\ldots,a,\xi,\ldots)=\exp(G_g)\ , \tag{3.14}$$

where G_g is the generator defined by Eqs. (3.12) and (3.13). (This manifold turns out to be the same one we defined in Ref. 10.) The important property of this manifold which allows us to use it to analyze the large-scale behavior is that it is closed under the space- and time-coarsening transformations S and T and the rescaling transformation R. A great virtue of the present (exponential) approach is that it makes this obvious, and makes it easy to determine the action of S, T, and R on the parameters $D_m,a,\xi,\ldots$. The action of T is particularly simple. Time-coarsening an exponential EOM [Eq. (3.7)] gives the product

$$T(\exp(E_g))=\exp(E_g)\exp(E_g)=\exp(2E_g)\ . \tag{3.15}$$

The action of T on a generator is therefore [using Eq. (3.6)]

$$T:\ G_g\to 2G_g\ . \tag{3.16}$$

Our collection of generators is obviously closed under this transformation. The necessary transformation of the D's is evidently [from Eq. (3.12)]

$$T:\ D_m\to 2D_m\ , \tag{3.17a}$$

and from Eq. (3.13) for the fluctuation generator we obtain

$$T:\ a\to 2a\ , \tag{3.17b}$$

$$T:\ \xi\to\xi\ . \tag{3.17c}$$

The actions of R and S are best seen in the limit that the generator G_g is infinitesimal; the results will extend to all G_g by repeated time-coarsening. Then $\exp(G_g)\sim 1_E+G_g$, and S and R act on generating propagators exactly as they do on the EOM propagators themselves; this action is given by Eq. (2.7) for R and Eq. (2.9) for S. It can be seen that R has no effect on the single-particle propagator [Eq. (3.12)],

$$R:\ D_m\to D_m\ , \tag{3.18a}$$

but from Eq. (3.13),

$$R:\ a\to a/4\ , \tag{3.18b}$$

$$R:\ \xi\to\xi\ . \tag{3.18c}$$

For space coarsening, Eq. (2.10) implies

$$S:\ (-D_0-D_2k^2-\cdots)\to(-D_0-D_2(k/2)^2-\cdots)\ , \tag{3.19}$$

so that

$$S:\ D_m\to 2^{-m}D_m\ , \tag{3.20a}$$

and Eq. (3.13) gives

$$S:\ a\to 2^{d-2}a\ , \tag{3.20b}$$

$$S:\ \xi\to\xi/2\ . \tag{3.20c}$$

Let us now try to generate an invariant manifold for our two-component system. Construct a generating EOM by simply combining the generators [Eqs. (3.12) and (3.13)] for the respective one-component systems,

$$G^e_e(k)=-D^e_0-D^e_2k^2-D^e_4k^4-\cdots\ , \tag{3.21a}$$

$$G^s_s(k)=-D^s_0-D^s_2k^2-\cdots\ , \tag{3.21b}$$

$$G^{ee}(k)=a^ek^2\exp(-\xi_e^2k^2-\cdots)\ , \tag{3.21c}$$

$$G^{ss}(k)=a^sk^2\exp(-\xi_s^2k^2-\cdots)\ . \tag{3.21d}$$

Clearly, this gives a manifold of EOM's in which the two species diffuse independently of one another. The simplest sort of interaction would involve including in the generator

$$G^e_s(k)=-D^{es}_0-D^{es}_2k^2+\cdots\ . \tag{3.22}$$

Then the coefficient $[c^e(r,1)]_{c^s(r,0)}$ describing the influence of the s content on the e content is nonzero. Thus extra electrons appear in numbers proportional to the number of s's: The s's act as mobile sources of electrons if $D^{es}_0\neq 0$. If $D^{es}_0=0$, but $D^{es}_2\neq 0$, electron-hole quadrupoles (e.g., spherical distributions with holes inside and electrons outside) are emitted.

The simplest nonlinear interaction is generated by the propagator depicted in Fig. 1(c),

$$G^e_{es}(k,q)=-B_0-Bk^2-B_2k(k-q)-B_3q^2-\cdots\ . \tag{3.23}$$

If $B_0>0$, electrons disappear in proportion to the product of the electron density and the s density; this reaction kinetics implies that the s's are traps for the electrons. If $B_0<0$, e's are appearing instead of disappearing, and therefore the s's can be interpreted as replicase enzymes for copying e's. If $B_0=0$, but $B>0$ we can describe the interaction as a modulation of the electron diffusivity proportionately to the local s content: We show in Sec. VI that the effective diffusivity D^e changes by c^sB. Thus we can think of the s's as (forward) scatterers (backward if $B<0$), and B as the scattering strength.

We have now uniquely defined a rather large invariant manifold of EOM's for a two-component system, each of which is obtained by exponentiating a generating EOM E_g defined by Eqs. (3.21)—(3.23). The manifold is parametrized by a fairly large number of parameters $(D^e_m,D^s_m,B,a^e,\xi_e^2,\ldots)$. For brevity, let us denote these by $(p_1,p_2,\ldots)=p$. Then we can write an arbitrary member of the manifold as $E(p)$. In the Markovian (large-D^α_2) limit we have been using, we can define the action of S on p by

$$E(Sp)=SE(p)\ , \tag{3.24}$$

and similarly for T and R_α. We have already computed Tp, Rp, and Sp for a one-component system [Eqs. (3.17)—(3.20)]; we can generalize these equations to a two-component system merely by putting α superscripts on D and a, and α subscripts on R and ξ. We extend the manifold to small D^α_2 by assuming (3.24) holds for all p; an explicit definition is

$$E(p)=\lim_{n\to\infty} S^n E(S^{-n}p) \ . \tag{3.25}$$

This gives the E for a small D_2^α in terms of the E for $S^{-n}D_2^\alpha = 2^{2n}D_2^\alpha$, which is large.

IV. FIXED POINTS AND THEIR VICINITIES

We would like to identify a family of fixed points among the two-component EOM's which is analogous to the family of diffusive fixed points parametrized by D_2^e and A^e which was found[10] for the one-component electron system under the combined coarsening transformation $ST^2R_e^{d/2}$. Evidently, the two-component EOM generated by Eqs. (3.21) with nonzero parameters D_2^e, D_2^s, a^e, a^s is fixed under $ST^2R^{d/2}$, where

$$R \equiv R_e R_s \ , \tag{4.1}$$

since this acts like $ST^2R_e^{d/2}$ on the electron propagator and like $ST^2R_s^{d/2}$ on the s propagator. Let us use $A^\alpha = a^\alpha/2D_2^\alpha$ [Eq. (3.11)] instead of a^α to describe the fluctuations: There is a four-parameter family of diffusive (Fick's-law) fixed points parametrized by D_2^e, D_2^s, A^e, and A^s in the invariant manifold for a two-component system. As in any system,[10] the large-scale behavior is determined by the coarsening behavior of the EOM's near a fixed point. In particular, the dominant corrections to diffusive large-scale behavior are determined by the largest eigenvalues of the coarsening transformation $ST^2R^{d/2}$ linearized near the fixed point. A very useful feature of the parametrized invariant manifold we have defined is that by perturbing the parameters (D_2^e, D_2^s, D_4^e, B, etc.) one at a time, we obtain instant eigenvectors of S, T, and R. This is because the transformations do not couple the parameters. The actions of the transformations on D_m^α are given by Eqs. (3.17)—(3.20), from which we deduce, for example, $ST^2R^{d/2}$: $D_0^e \to 2^2 D_0^e$. A perturbation from the fixed point with nonzero decay rate D_0^e is unstable; it is moved 4 times farther from the fixed point by the transformation, i.e., the corresponding eigenvalue is 4. However, this corresponds to a nonconservative system and will not arise in the systems we consider. A perturbation involving changing the diffusivity D_2^e is unchanged by the transformation $ST^2R^{d/2}$: $D_2^e \to D_2^e$, so that the corresponding eigenvalue is 1 (such an eigenvector is called "marginal" in the language of critical phenomena[13]). The eigenvalue for the Burnett coefficient D_4^e is 2^{-2}; this was the largest eigenvalue we found for the one-component system,[10] which therefore determined the large-scale behavior of such a system. In the two-component system, however, the coarsening rules (Sec. II) imply, for the scattering strength B [Eq. (3.23)],

$$\begin{aligned} &S\text{: } B \to 2^{-d-2}B \ , \\ &T\text{: } B \to 2B \ , \\ &R_e\text{: } B \to B \ , \\ &R_s\text{: } B \to 2B \ , \end{aligned} \tag{4.2}$$

so that

$$ST^2R^{d/2}\text{: } B \to 2^{-d/2}B \ . \tag{4.3}$$

The eigenvalue for B is $2^{-d/2}$, larger than the previously dominant one if $d<4$. (The sources and traps [Eqs. (3.22) and (3.23)] give still larger eigenvalues, but we consider only electron-conserving systems here.)

The large-scale behavior of an interacting two-component system in one, two, and three dimensions will thus be dominated by the effects of this eigenvector; it is therefore the main objective of this paper to determine these effects.

V. LARGE-SCALE BEHAVIOR OF A SYSTEM WITH SCATTERERS

We now know the fixed points of the coarsening transformation $ST^2R^{d/2}$ and some of the eigenfunctions and eigenvalues of the linearized transformation. Let us then suppose we have a two-component diffusive system described microscopically by a certain EOM, which we have coarsened with $ST^2R^{d/2}$ until it is close enough to a fixed point that only one eigenfunction has significant amplitude. This will be the one with the largest eigenvalue ($2^{-d/2}$), whose amplitude is the scattering strength denoted by B in Eq. (3.23). The fixed point we approach is uniquely specified by the electron and scatterer diffusivities D^e and D^s (from now on we will omit the subscript 2), and by the mean-square fluctuations in electron and scatterer densities A^e and A^s [Eq. (3.2)]. It turns out to be necessary to allow one additional nonzero parameter describing the scatterer fluctuations, namely their correlation length ξ_s, because the fixed-point limit $\xi_s \to 0$ is singular in a certain sense.

We would like to calculate some experimentally measurable properties of this system with scatterers. We will concentrate on the dynamic structure factor $S(q,\omega)$ for the electrons, which is determined by the equilibrium unequal-time averages $G_{\rm eq}^{ee}(k,1,-k,0)$. These can be regarded as "EOM coefficients" in the equilibrium ensemble, and can be calculated by the ensemble-changing procedure of Appendix C from the EOM coefficients (such as G^{ee}) in the smaller ensemble in which all variables at times $t \le 0$ are constrained. This procedure essentially amounts to averaging over the possible fluctuations of these $t \le 0$ variables. One can do this in two stages: First, average over the scatterer fluctuations (i.e., convert to an ensemble in which only the electron contents are fixed at $t \le 0$) via graphs such as those in Fig. 5, and then, average over the electron fluctuations using the graphs in Fig. 6. It can be seen that the latter averaging is uninteresting in our case; we have only Fig. 6(a), in which there is only one graph. It tells us that the unequal-time average is obtained by convoluting the propagator G_e^e with the equal-time average $G_{\rm eq}^{ee}$ [which is in fact nearly independent of k for small ξ; see Eq. (5.2)]. We have

$$G_{\rm eq}^{ee}(k,1,-k,0) = G_e^e(k) G_{\rm eq}^{ee}(k,0,-k,0) \ . \tag{5.1}$$

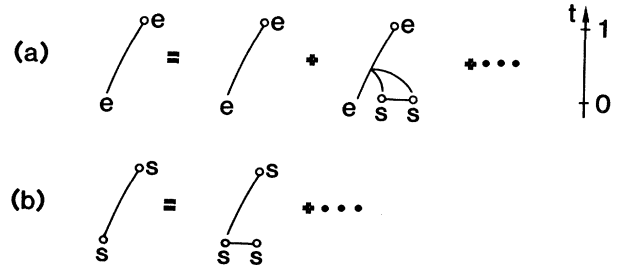

FIG. 5. Graphs for averaging the EOM coefficients over the scatterer contents (described in Appendix C). They involve averaging over all values $c^s(\ldots,0)$ of the scatterer content at $t=0$.

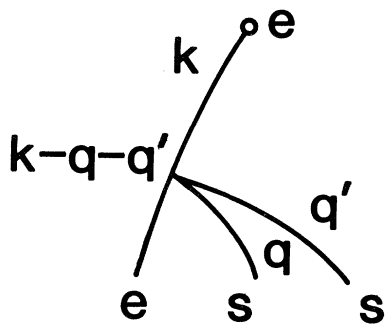

FIG. 7. Wave-vector labeling for the quadratic scattering propagator $G^e_{ess}(k,q,q')$ [Eq. (5.4)].

This really contains no more information than the propagator did. [If we chose to allow electron-electron interactions, we would have nontrivial graphs like Fig. 6(b).]

Thus, the physics is all contained in Fig. 5(a), which gives the scatterer-averaged electron propagator (denoted by a prime: $[G^e_e(k)]'$) in terms of the fixed-scatterer propagator $G^e_e(k)$ and a correction term involving the interaction propagator quadratic in the scatterer density, $G^e_{ess}(k,q,q')$ (the wave vector labeling is indicated in Fig. 7). We must therefore calculate these unprimed propagators for our EOM in the invariant manifold, whose generating EOM is given by Eqs (3.21) and (3.23) with nonzero D^e, D^s, a^e, a^s, ξ_s, and B. We will compute the exponential [Eq. (3.7)] perturbatively in B using the method of Appendix E. We will take the unperturbed EOM e^E this time to be the fixed-point EOM parametrized by D^e, D^s, A^e, and A^s, except we will also allow the scatterer correlation length $\xi_s>0$. This modifies Eq. (3.9b) by a factor $\exp(-\xi_s^2k^2)$,

$$G^{ss}(k)=A^s\exp(-\xi_s^2k^2)[1-\exp(-2D^sk^2)]\ , \qquad (5.2a)$$

leading to a similar modification of the equilibrium average,

$$G^{ss}_{\rm eq}(k)=A^s\exp(-\xi_s^2k^2)\ . \qquad (5.2b)$$

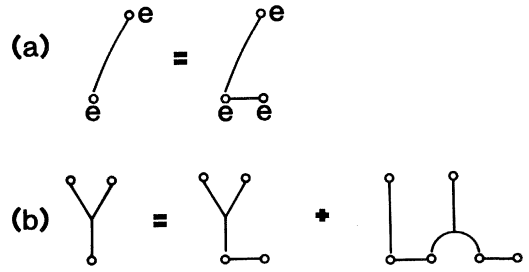

FIG. 6. Graphs for computing equilibrium averages from scatterer-averaged EOM coefficients by averaging over electron contents $c^e(\ldots,0)$. Species labels are all e and are omitted in (b).

The perturbation generator E will be the B term of Eq. (3.23), i.e., the scattering. The rules listed in Appendix E then lead to the topological graphs shown in Fig. 8. These have simple physical interpretations: In the second term of Fig. 8(a) an electron diffuses until time u, when it interacts with a scatterer fluctuation. Both it and the scatterer diffuse until time u', when they interact again, after which the electron diffuses until (dimensionless) time 1. Applying the evaluation rules (Appendix E) to Fig. 8(a) gives the invariant-manifold electron propagator to order B^2,

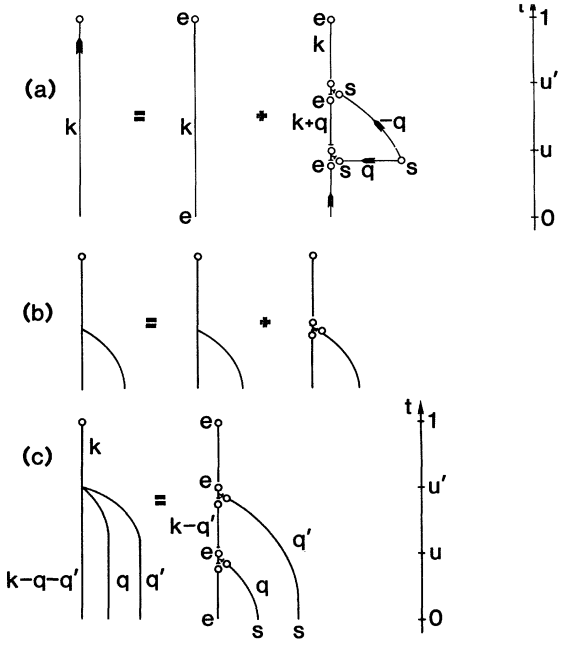

FIG. 8. Graphs for computing invariant-manifold propagators (left-hand sides) perturbatively using the method of Appendix E. In the composite graphs on the right-hand sides of the equations, subgraphs with the shortest ("infinitesimal") arms represent the perturbation generator F, and those with longer arms represent the exponentiated unperturbed EOM acting over a time interval Δu, $e^{E\Delta u}$. (E and F here are different from those in Fig. 3.)

$$G_e^e(k)=\exp(-D^e k^2)+\int_0^1 du\int_u^1 du'(2\pi)^{-d}\int dq\,\exp(-D^e k^2 u)A^s\exp(-\xi_s^2 k^2)[1-\exp(-2D^s q^2 u)]$$
$$\times[-B(k+q)^2]\exp[-D^e(k+q)^2(u'-u)]\exp[-D^s q^2(u'-u)](-Bk^2)$$
$$\times\exp[-D^e k^2(1-u')]\ . \tag{5.3}$$

The factors in the integrand are just the propagators in Fig. 8(a), reading upward. The factor involving A^s is the conditional scatterer fluctuation G^{ss} [Eq (5.2a)], part of the unperturbed EOM for propagating from time 0 to time u, which is represented by the horizontal line in Fig. 8(a). Each factor involving B is an interaction generator [Eq. (3.23)], represented by a three-armed subgraph. The interaction propagator $G_{es}^e(k,q)$ can be calculated similarly [Fig. 8(b)]. The first graph on the right-hand side is the unperturbed ($B=0$) G_{es}^e, which vanishes; we therefore omit the corresponding graph in Fig. 8(c), which is the other propagator we need for the scatterer-averaged EOM (Fig. 5), $G_{ess}^e(k,q,q')$. This is of second order in B; algebraically,

$$G_{ess}^e(k,q,q')=\int_0^1 du\int_u^1 du'\exp[-uD^e(k-q-q')^2][-B(k-q')^2]$$
$$\times\exp[-(u'-u)D^e(k-q)^2](-Bk^2)\exp[-(1-u')D^e k^2-uD^s q^2-u'D^s q^2]\ . \tag{5.4}$$

We now return to Fig. 5(a) to calculate the scatterer-averaged electron propagator. The wave vectors in Fig 5(a) are to be labeled as in Fig. 7, but with $q'=-q$. The rules of Appendix C give

$$G_e^e(k)'=G_e^e(k)+(2\pi)^{-d}\int dq\,G_{ess}^e(k,q,-q)G_{\rm eq}^{ss}(q)\ . \tag{5.5}$$

Writing the integral in Eq. (5.5) explicitly [using Eqs. (5.4) and (5.2b)], we see that it exactly cancels with part of the first term $G_e^e(k)$ [obtained from Eq. (5.3)], namely the term proportional to $\exp(-2D^s q^2 u)$. (Physically, this is because the decay of fluctuations during u must exactly cancel their generation to maintain equilibrium.) The remainder of Eq. (5.3) is therefore our final result for the scatterer-averaged propagator $G_e^e(k')$. As we have observed in Eq. (5.1), this is essentially the electron time correlation function, from which the inelastic scattering function $S(k_p,\omega_p)$ could be obtained by converting to the physical variables (k_p, D_p^e, etc.) and Fourier-transforming in Δt.

In this paper we will examine the mean-square displacement (at $t=1$, i.e., $t_p=\Delta t$) which involves the $k=0$ limit only. From the remaining term of Eq. (5.3),

$$\langle r^2\rangle=-\nabla_k^2 G_e^e(k=0)'=2dD^e-2dB^2A^s(2\pi)^{-d}\int d^dq\,q^2\int_0^1 du\int_u^1 du'\exp[-(u'-u)(D^e+D^s)q^2-\xi^2q^2]\ , \tag{5.6}$$

where we have dropped the subscript from ξ, the scatterer correlation length. Note that the second term of Eq. (5.6) depends only on the sum D^e+D^s, which we will denote by D. Thus the behavior of a system with diffusing scatterers is not qualitatively different from that of a system with frozen disorder. Equation (5.6) can be integrated exactly, giving, for $d=1$,

$$\langle r^2\rangle_{d=1}=2D^e-\pi^{-1/2}B^2A^sD^{-2}[(D/\xi)+2\xi-2(\xi^2+D)^{1/2}]\ . \tag{5.7}$$

To see the actual time dependence, we must express this in terms of physical rather than dimensionless quantities. The physical time interval is Δt and the physical displacement is

$$r_p=r\,\Delta r\ . \tag{5.8}$$

The physical diffusivities are

$$D_p^\alpha=D^\alpha(\Delta r)^2/\Delta t\ , \tag{5.9}$$

where the correct factors of Δr, Δt, and Δc^α can be determined[14] by requiring the physical quantities to be invariant under S, T, and R. Applying this criterion to B and A^α gives

$$B_p=B(\Delta r)^{d+2}/\Delta t\,\Delta c^s\ , \tag{5.10}$$

$$A_p^\alpha=A^\alpha(\Delta r)^{-d}(\Delta c^\alpha)^2\ , \tag{5.11}$$

$$\xi_p^\alpha=\xi^\alpha\Delta r\ , \tag{5.12}$$

using Eqs. (4.2), (3.18), and (3.20). Thus the physical mean-square displacement after a time Δt is

$$\langle r_p^2(\Delta t)\rangle_{d=1}=2D_p^e\Delta t-\pi^{1/2}B_p^2A_p^sD_p^{-2}[(D_p\,\Delta t/\xi_p)+2\xi_p-2(\xi_p^2+D_p\,\Delta t)^{1/2}]\ . \tag{5.13}$$

This expression is exact to second order in B_p, in the limit of large D^α for which the continuum-limit exponential form of the invariant-manifold EOM holds without the need for space-coarsening [Eq. (3.25)]. In practical terms, this means Eq. (5.13) may have corrections of relative order $1/D^\alpha$, i.e., $(\Delta t)^{-1}$.

VI. MEAN-SQUARE DISPLACEMENT AT LONG TIMES IN ONE DIMENSION

In the limit of long times (and/or short correlation lengths: $\Delta t \gg \xi_p^2/D_p$), the mean-square displacement [Eq (5.13)] becomes

$$\langle r_p^2(\Delta t)\rangle_{d=1} = 2D_p' \Delta t + 2\pi^{-1/2} B_p^2 A_p^s (D_p)^{-3/2} \Delta t^{1/2} , \tag{6.1}$$

where the effective diffusion coefficient is

$$D_p' = D_p^e - 2^{-1}\pi^{-1/2} B_p^2 A_p^s / D_p \xi_p . \tag{6.2}$$

It is now apparent why we had to allow $\xi \neq 0$: The electron diffusivity undergoes an infinite renormalization ("ultraviolet divergence") in the limit of zero scatterer correlation length.

These results agree with those obtained by other workers for specific disordered one-dimensional systems. To apply it to a specific system, one must determine the values of the coefficients D_p^e and A_p^s describing the diffusive fixed point which the system approaches under the coarsening transformation $ST^2R^{d/2}$, and the values of the scatterer correlation length ξ_p and the scattering strength B_p describing its distance from the fixed point. We will do this explicitly for the most frequently studied[1,7,8] disordered random walk. This is a walk (of electrons, for instance) on a regular lattice of sites separated by l in which the jump rate W between two sites is a random variable fluctuating (independently of the rates for other bonds) about a mean value W_0: $\delta W = W - W_0$. On a microscopic ($\Delta r = l$) scale, δW plays the role of the "scatterer," and we may as well set the scatterer content c_p^s equal to δW. (There is a technical complication due to the fact that the scatterer and electron contents are most naturally defined in cells displaced by $\frac{1}{2}$, but this has no macroscopic consequences.) We are free to choose the unit of scatterer content; the simplest choice is $\Delta c^s = W_0$. It is well known[8] that the diffusivity of this system in the absence of scatterers (i.e., with $\delta W = 0$) is

$$D_p^e = l^2 W_0 . \tag{6.3}$$

We can relate the fluctuation $\langle \delta W^2 \rangle$ to our parameter A^s by integrating Eq. (2.5) over k' and using Eq. (3.2),

$$A^s = G_{\rm eq}^{ss}(k=0) = \sum_r \langle c^s(r,0) c^s(r',0)\rangle , \tag{6.4}$$

so we obtain

$$A_p^s = \langle \delta W^2 \rangle / l^d . \tag{6.5}$$

To determine the interaction strength B, it is easiest to consider a system having a uniform scatterer density c^s, i.e., a uniform δW. The scatterer-averaged electron propagator (Appendix C) is then

$$G_e^e(k) = \exp(-D^e k^2 - B c^s k^2) , \tag{6.6}$$

so that the scatterers increase the effective diffusivity to $D^e + Bc^s$. The change in the physical diffusivity [Eqs. (5.9) and (5.10)] is $B_p c_p^s / l^d$; equating this to the known diffusivity increase $l^2 \delta W$ of the microscopic model gives

$$B_p = l^{2+d} . \tag{6.7}$$

We can now calculate the mean-square displacement (Eq. 6.1),

$$\langle r_p^2(\Delta t)\rangle_{d=1} = 2D_p' \Delta t + 2\pi^{-1/2} l^2 W_0^{1/2} (\langle \delta W^2 \rangle / W_0^2)(\Delta t)^{1/2} , \tag{6.8}$$

and the coefficient of $\Delta t^{1/2}$ is identical to that obtained by exact solution of this model for weak disorder.[7] The effective diffusivity D_p' [Eq. (6.2)] is harder to obtain for this model since it is not obvious what to use for ξ_p. Evidently, it should be of order l; the exact result is reproduced if we choose $\xi_p = l/2\pi^{1/2}$.

The renormalization-group idea has been applied previously to this model by Machta[8] from quite a different point of view. Machta took a site-decimation approach rather than the present cell-lumping approach. The dynamics was described by a waiting-time distribution, which can, in principle, be renormalized by computing the waiting-time distribution for a double jump of length $2l$. The renormalized waiting-time distribution is very difficult to compute, however, and in Ref 8 only the zero-frequency component was actually renormalized. This describes the approach to the fixed point correctly, but will not correctly describe the system on a microscopic ($\Delta r = 2l$, $4l$, etc.) scale. The present approach has the advantage of being able to renormalize an equation of motion accurately on any scale (this has not been done for small scales in the present paper, but see Ref. 11) One can follow in detail the renormalization trajectory of a system from the microscopic scale to the fixed point.

Another advantage of our discrete-hydrodynamics method is that it works in any dimensionality; the decimation approach does not straightforwardly generalize to $d > 1$. In the next section we present the results for $d = 2$ and 3.

VII. MEAN-SQUARE DISPLACEMENT IN TWO AND THREE DIMENSIONS

The formula for mean-square displacement [Eq (5.6)] can be integrated for $d = 2$, giving

$$\langle r_p^2(\Delta t)\rangle_{d=2} = 4D_p^e \Delta t - B_p^2 A_p^s \frac{1}{\pi D_p^2} [D_p \xi_p^{-2} \Delta t - \ln(1 + D_p \Delta t / \xi_p^2)] . \tag{7.1}$$

Again there is a nonanalytic term at long times ($\Delta t \gg \xi_p^2/D_p$), and this time it is a logarithm

$$\langle r_p^2(\Delta t)\rangle_{d=2} = 4D_p' \Delta t + \pi^{-1} B_p^2 A_p^s D_p^{-2} \ln(D_p \Delta t / \xi_p^2) , \tag{7.2}$$

where the renormalized diffusivity is

$$D_p' = D_p^e - B_p^2 A_p^s / 4\pi \xi_p^2 D_p . \tag{7.3}$$

Corrections to Eq. (7.2) should be of order $(\Delta t)^0$ or smaller. For the two-dimensional (2D) version of the disordered random-walk model of Sec. VI, the $\ln(\Delta t)$ term in Eq. (7.2) is

$$\pi^{-1}l^2(\langle \delta W^2\rangle / W_0^2)\ln(\Delta t)\ . \tag{7.4}$$

This model has not been solved exactly, but has been studied in an effective-medium approximation by Haus, Kehr, and Kitahara.[15,16] From their effective waiting-time distribution $W(t)$, one can calculate the mean-square displacement [the inverse Laplace transform of $2dW(s)/s^2$]. For the case of weak disorder the nonanalytic term reduces exactly to expression (7.4).

In three dimensions, the mean-square displacement (Eq. 5.6) gives

$$\langle r_p^2(\Delta t)\rangle_{d=3}=6D_p^e\,\Delta t-(3/4\pi^{3/2})B_p^2A_p^sD_p^{-2}[\xi_p^{-3}D_p\,\Delta t-2\xi_p^{-1}+2(\xi_p^2+D_p\,\Delta t)^{-1/2}]\ , \tag{7.5}$$

so that the effective diffusivity is

$$D_p'=D_p^e-B_p^2A_p^s/8\pi^{3/2}\xi_p^3D_p\ , \tag{7.6}$$

and for long times,

$$\langle r_p^2(\Delta t)\rangle_{d=3}=6D_p'\,\Delta t+(3/2\pi^{3/2})B_p^2A_s^pD_p^{-2}\xi_p^{-1}(\Delta t)^0+(3/2\pi^{3/2})B_p^2A_p^s(D_p)^{-5/2}(\Delta t)^{-1/2} \tag{7.7}$$

For the random-walk model of Sec. VI, the $(\Delta t)^{-1/2}$ term of Eq. (7.7) is

$$\tfrac{3}{2}\pi^{-3/2}l^2W_0^{-1/2}(\langle \delta W^2\rangle / W_0^2)(\Delta t)^{-1/2}\ . \tag{7.8}$$

This has also been estimated in an effective-medium approximation by Haus *et al.*;[16] their result reduces in the limit of weak disorder exactly to Eq. (7.8). Thus the effective-medium approximation gives the leading nonanalytic long-time behavior exactly for $d=3$ and 2; this was previously known for $d=1$ [the $(\Delta t)^{1/2}$ term].[7,17–19]

VIII. CONCLUSIONS

Using a discrete formulation of hydrodynamics, we have identified the fixed points of a scale-coarsening transformation which govern the large-scale behavior of diffusive systems. The eigenfunctions of the linearized transformation which modify this behavior in disordered systems have also been calculated exactly. The known nonanalytic behavior in one dimension was exactly reproduced, and the behavior in two and three dimensions was determined.

The problem of nonanalyticity ("long-time tails") in disordered systems is closely related to the corresponding problem in fluids. It is hoped that the identification of the exact fixed points and eigenfunctions for a fluid system will facilitate the calculation of transport properties of dense fluids by the numerical coarsening of small-scale equations of motion.[12,20]

Other problems which may be susceptible to attack from this point of view are transport in a disordered system subject to a uniform field[21] [by including a term of order k in Eq. (3.21a)] and diffusion in materials with traps.[22]

ACKNOWLEDGMENTS

The author is indebted to Professor J. P. Straley for useful conversations and for pointing out a sign error in Eq. (7.7), which has since then been rectified. This work was supported by the Chemistry Division of the National Science Foundation under Grant No. CHE-81-06122.

APPENDIX A: DERIVATION OF GRAPHICAL RULES FOR TIME-COARSENING MARKOVIAN DYNAMIC EOM'S

Let us first look at the problem of time-coarsening the general discrete EOM discussed in Sec. II. A very general solution to this problem was derived in Ref. 11, which was used to iterate the coarsening transformation numerically. That result was more general than we need for the present purpose in two ways. First, variables were defined at half-integer values of t ("transfers"), as well as at integer values ("contents"). The former are not used in the present formulation and complicate the calculation considerably. Second, the EOM was allowed to be non-Markovian, whereas in the present case we are considering the continuous-space limit in which the EOM is Markovian (the contents at $t=1$ depend only on those at $t=0$). We will therefore give here a simplified rederivation of the time-coarsening equations, valid for Markovian EOM's for the cell contents; we will not assume the continuous-space limit.

Let us suppose that we know the discrete equation of motion coefficients,

$$[c(r,1)c(r',1)\cdots]_{c(\bar{r},0)c(\bar{r}',0)\cdots}\ , \tag{A1}$$

such as those in Eq. (2.2), describing a system on the time scale Δt. (The species index α plays no role here, and so we will not write it explicitly.) These give the moments of the c's at time $t=1$ in an ensemble in which they are fixed at $t\le 0$; they are identical to the coefficients

$$[c(r,2)\cdots]_{c(\bar{r},1)\cdots} \tag{A2}$$

describing the moments at $t=2$ in the ensemble fixed at $t\le 1$, because our system is stationary. We wish to compute the time-coarsened EOM coefficients

$$[c(r,2)\cdots]_{c(\bar{r},0)\cdots} \tag{A3}$$

describing evolution over the larger time interval $2\Delta t$. Note that coefficients (A3) describe the same ensemble as coefficients (A1), namely that in which the contents are fixed at $t\le 0$ (it is true that one has contents fixed at $t=-1$ and the other does not, but in our Markovian system the moments do not depend on times $t<0$). This ensemble is larger than the ensemble described by the coeffi-

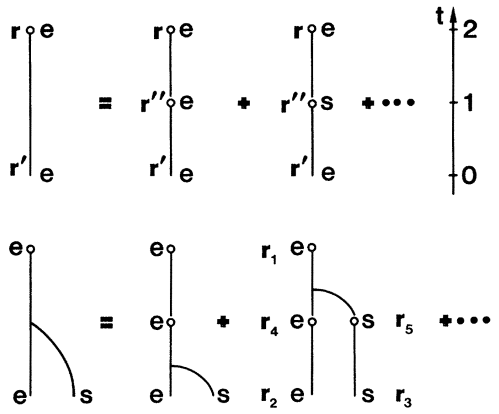

FIG. 9. Graphs for time-coarsening an EOM. Time t increases upward. Vertices representing contents $c^{\alpha}(r,t)$ are labeled by position r and species index α (equal to e or s).

cients (A2), in which contents at $t=1$ are also fixed. We are therefore faced with computing EOM coefficients [moments of $c(r,2)$] in a larger ensemble [Eq. (A3)] from those in a smaller ensemble [Eq. (A2)]. This is precisely the ensemble-changing problem addressed in general in Appendix C. The solution obtained there is depicted graphically in Fig. 9. The top equation of Fig. 9 corresponds to

$$[c^e(r,2)]_{c^e(r',0)} = \sum_{r''} [c^e(r,2)]_{c^e(r'',1)} [c^e(r'',1)]_{c^e(r',0)} + \sum_{r''} [c^e(r,2)]_{c^s(r'',1)} [c^s(r'',1)]_{c^e(r'',0)} , \tag{A4}$$

according to the rules described in Appendix C. The graphs can also be interpreted in Fourier space, labeling the arms by k vectors as in Fig. 2. The rules for writing the corresponding algebraic expression in k space [the Fourier transform of Eq. (A4)] are given in Appendix D; they lead to Eq. (2.11).

APPENDIX B: MULTIPLYING MARKOVIAN EOM'S

In Appendix A we developed graphical rules for time-coarsening Markovian EOM's by combining propagators between $t=0$ and 1 with those between 1 and 2. We now note that these two EOM's need not have been the same. We could have used any two EOM's, for instance, E_a and E_b; in each coarsening graph (for example Fig. 2), each lower EOM graph (previously connecting times 0 and 1) would represent a propagator of E_a, and each upper EOM graph (previously connecting $t=1$ to $t=2$) would represent a propagator of E_b. The graphical procedure [or Eq. (C7)] would then give us the propagators of a new EOM which we may denote $E_b E_a$. We have thereby defined the product of an arbitrary pair of Markovian EOM's.

APPENDIX C: GRAPHICAL METHOD FOR ENSEMBLE-CHANGING

We will describe a graphical procedure which can be used to compute EOM coefficients such as

$$[c(r,t)c(r',t)\cdots]_{c(r'',0)\cdots}$$

in a large ensemble L from those in a smaller ensemble S (i.e., one in which more variables are constrained). Essentially, this method (but without the graphs) was used in Refs. 23 and 11. We apply the method in Appendix A to the case where the large ensemble L is that in which all variables are fixed for $t \le 0$, and in S they are fixed for $t=1$ as well. In Sec. III we consider principally the case where the small ensemble S is the one in which all variables (c^e and c^s) are fixed for $t \le 0$, and L is the equilibrium ensemble; Sec. V involves yet another choice. Here we will describe the method for an arbitrary choice of L and S.

Three types of content variables are involved: those which are predicted (i.e., not constrained) in both ensembles, which we denote by p, those constrained in the small ensemble S but predicted in the large ensemble L, denoted f because they fluctuate in L, and those constrained in both S and L, denoted c [not to be confused with the symbol for content, $c(r,t)$]. Thus in the case of Appendix A, p is $c(r,2)$, f is $c(r,1)$, and c is $c(r,0)$.

The EOM coefficents in the L ensemble describe the moments of the predicted variables p and f as functions of the constrained variables c. Using a concise notation in which a $\underline{p}$, $\underline{f}$, or $\underline{c}$ denotes a product of variables of that type, the power-series expansion of a general moment is

$$[\underline{p}\,\underline{f}]^L = \sum_{\underline{c}} [\underline{p}\,\underline{f}]^L_{\underline{c}} \underline{c} , \tag{C1}$$

which defines the EOM coefficients $[\underline{p}\,\underline{f}]^L_{\underline{c}}$. A superscript L (S) indicates that the EOM coefficient describes the large (small) ensemble, and the sum is over all products $\underline{c}$ of constrained variables. The corresponding expression for the small ensemble is

$$[\underline{p}]^S = \sum_{\underline{c},\underline{f}} [\underline{p}]^S_{\underline{c}\,\underline{f}} \underline{c}\,\underline{f} . \tag{C2}$$

We can relate the L and S coefficients by averaging Eq. (C2) over the large ensemble

$$[[\underline{p}]^S]^L = [\underline{p}]^L = \sum_{\underline{c},\underline{f}} [\underline{p}]^S_{\underline{c}\,\underline{f}} \underline{c} [\underline{f}]^L . \tag{C3}$$

Using Eq. (C1) to express $[\underline{f}]^L$ in terms of $\underline{c}$'s, we can make a comparison to the expansion [Eq. (C1)] of $[\underline{p}]^L$ to identify the EOM coefficients,

$$[\underline{p}]^L_{\underline{c}} = \sum_{\underline{f}} \sum_{\text{fact}} [\underline{p}]^S_{\underline{c}'\underline{f}} [\underline{f}]^L_{\underline{c}''} . \tag{C4}$$

The inner sum is over all factorizations of the product $\underline{c}$ into two products $\underline{c}'\underline{c}''$; note that $\underline{c}'=\underline{c},\underline{c}''=1$ or $\underline{c}''=\underline{c},\underline{c}'=1$ is allowed, as is $\underline{f}=1$. As an example, we write Eq. (C4) explicitly for the case in which $\underline{p}$ and $\underline{c}$ are products of one variable only:

$$[p]_c^L=[p]_c^S+\sum_f([p]_f^S[f]_c^L+[p]_{fc}^S[f]_1^L)$$
$$+\sum_{f,f'}([p]_{ff'}^S[ff']_c^L+[p]_{ff'c}^S[ff']_1^L)\ . \qquad \text{(C5)}$$

Equation (C4) is one form of the desired relation between L and S coefficients. However, in practice, we must[23,11] deal with cumulant moments $[\underline{p}]^{\text{cum}}$ defined inductively by

$$[\underline{p}]=\sum_{\text{fact}}[\underline{p}']^{\text{cum}}[\underline{p}'']^{\text{cum}}\cdots\ , \qquad \text{(C6)}$$

where we sum over all factorizations $\underline{p}'\underline{p}''\cdots=\underline{p}$. The correct form of Eq. (C4) in terms of cumulants is[11] (omitting the superscript "cum"—from now on all moments are cumulants)

$$[\underline{p}]_{\underline{c}}^L=\sum_{\underline{f}}\sum_{\text{fact}}[\underline{p}']_{\underline{c}'\underline{f}'}^S[\underline{p}'']_{\underline{c}''\underline{f}''}^S\cdots[\underline{\tilde{f}}']_{\tilde{c}'}^L[\underline{\tilde{f}}'']_{\tilde{c}''}^L\cdots\ . \qquad \text{(C7)}$$

Here, the inner sum is over factorizations $\underline{p}'\underline{p}''\cdots$ of $\underline{p}$, $\underline{c}'\underline{c}''\cdots\underline{\tilde{c}}'\cdots$ of $\underline{c}$, and over two *independent* factorizations $\underline{f}'\underline{f}''\cdots=\underline{f}$ and $\underline{\tilde{f}}'\underline{\tilde{f}}''\cdots=\underline{f}$ of $\underline{f}$. Each individual content factor f of $\underline{f}$ appears in one $[\ ]^S$ and one $[\ ]^L$, linking them; the sum includes only terms all of whose EOM factors are linked in this way. For our special case of one p and one c, the cumulant form of Eq. (C5) has the additional terms

$$+\sum_{f,f'}([p]_{ff'}^S[f]_1^L[f']_c^L$$
$$+[p]_{ff'}^S[f]_c^L[f']_1^L+[p]_{ff'c}^S[f]_1^L[f']_1^L)\ . \qquad \text{(C8)}$$

These equations are easiest to grasp graphically; a graphical representation of Eqs. (C5) and (C8) is shown in Fig. 10. Each EOM coefficient $[\ ]\ldots$ is represented by an "EOM graph"; the one on the left in Fig. 10 represents $[p]_c$. In general, an EOM graph has several arms which diverge from a central point. The central point is visible as a junction of three arms in the third graph on the right, representing $[p]_{cf}[f]$; $[p]_c$ should be thought of as having an upper and a lower arm which meet invisibly at the center. Each vertex (the end of an arm) which is decorated with a circle represents a predicted variable, and each undecorated vertex is a constrained variable (i.e., a subscript in $[c(r,t)\cdots]_{c(r',t')\ldots}$). The EOM graph representing $[f]$ in the third graph on the right has an arm of zero length; only the circle decorating the end is visible. The terms on the right in Fig. 10 are composite graphs each involving several EOM graphs, and represent products of the corresponding EOM coefficients. Where two vertices from two EOM graphs are drawn next to each other (e.g., at f in the second term on the right) they represent the same variable; we will refer to this as a single "internal" vertex. Exactly one of the two arms at an internal vertex will be decorated, since f must be predicted in one EOM graph and constrained in the other. Each internal vertex is to be summed over; this is indicated by a sum over f in Eq. (C5), meaning a sum over positions r and, if α is not specified on the graph as in Fig. 9, over α. The linkage condition on Eq. (C7) requires simply that a graph not fall apart, but be connected by internal vertices.

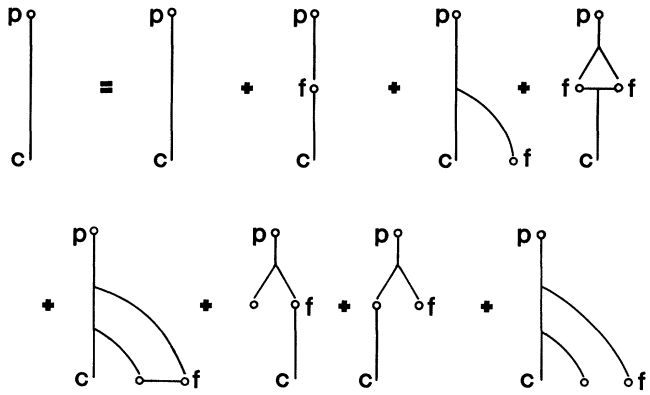

FIG. 10. Graphs representing Eqs. (C5) and (C8). The graph on the left-hand side represents an EOM coefficient $[p]_c^L$ in the L ensemble. On the right-hand side each EOM graph with a predicted (decorated) f vertex (the lower graphs here) describes the L ensemble, and the other ones describe the S ensemble.

Unlinked graphs must be omitted (actually you cannot even draw one unless $\underline{p}$ has more than one variable). All the graphs in Fig 10 vanish for the case dealt with in Sec. V, except the first and fifth terms which are included in Fig. 5(a). In Appendix A (T-coarsening) only the second term is nonzero; it appears as two graphs in Fig. 9 because the sum over α has been shown explicitly.

Equation (C7) can easily be generalized[11] to give $[\underline{p}\,\underline{f}]_{\underline{c}}^L$,

$$[\underline{p}\,\underline{\bar{f}}]_{\underline{c}}^L=\sum_{\underline{f}}\sum_{\text{fact}}[\underline{p}']_{\underline{c}'\underline{f}'}^S\cdots[\underline{\tilde{f}}'\underline{\bar{f}}']_{\tilde{c}'}^L\cdots\ , \qquad \text{(C9)}$$

where now $\underline{\bar{f}}$ is factorized as $\underline{\bar{f}}'\underline{\bar{f}}''\cdots$. Figure 5(b) is such a case, with $\underline{p}=c^s(r,1)$, $\underline{\bar{f}}=c^s(r',0)$, and $\underline{c}=1$. Figure 6 represents a different choice of L and S.

APPENDIX D: DERIVATION OF RULES FOR GRAPHICAL CALCULATION IN k SPACE

The ensemble-change equation (C7) used for time-coarsening (Appendix A) and scatterer-averaging (Sec. V) can be Fourier-transformed via Eqs. (2.4)—(2.6). We may represent the Fourier transforms

$$G_{\tilde{\alpha}\tilde{\alpha}'\cdots}^{\alpha\alpha'\cdots}(k,t,k',t',\ldots;\tilde{k},\tilde{t},\ldots)$$

by EOM graphs such as those of Appendix C. They have the meanings indicated in Fig. 1; a general G with N_p predicted variables (superscripts $\alpha\alpha'\cdots$) and n_c constrained ones (subscripts $\tilde{\alpha}\tilde{\alpha}'\cdots$) is represented by a graph with n_p+n_c arms intersecting at a single point, labeled by $k,k',\ldots,\tilde{k},\ldots$ The vertices at the ends may be labeled by the species index α; those corresponding to predicted variables are decorated by circles (these arms will usually point upwards). We must sometimes distinguish the G's describing the L ensemble from those of the S ensemble; in Sec. V these are called G' and G, respectively.

To see how to calculate such a Fourier transform graphically, consider an r-space graph such as Fig. 11(a) representing a term in the ensemble-change equation (C7). Suppose for concreteness we are time-coarsening so that the upper vertex involves time $t=2$ [$c^e(r_5,2)$, for instance]. The bottom vertices are $c^e(r_1,0)$ and $c^e(r_2,0)$, and the ones labeled r_3 and r_4 are at $t=1$ This term is a sum over r_3 and r_4 of a product of EOM coefficients, each of which can be expressed in terms of its Fourier transform [most generally, using Eq. (4.2) of Ref. 10]. The upper EOM graph, for example, is

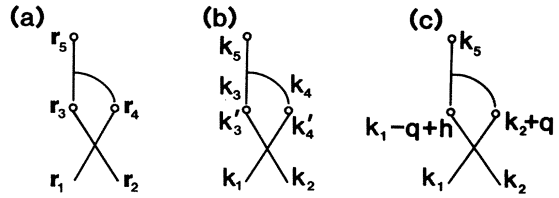

FIG. 11. (a) Fourier transformation of a graph of the type used in Eq. (C7) (e.g., for time-coarsening). The properly labeled k-space graph is (c). All vertices represent electrons, and so we omit the species label e.

$$[c^e(r_5,2)]_{c^e(r_3,1)c^e(r_4,1)}=\int\frac{dk_5}{(2\pi)^d}e^{ik_5r_5}\int\frac{dk_3}{(2\pi)^d}e^{-ik_3r_3}\int\frac{dk_4}{(2\pi)^d}e^{-ik_4r_4}(2\pi)^d\delta_{2\pi}(k_5-k_3-k_4)G^e_{ee}(k_5;k_3,k_4)\ . \tag{D1}$$

Multiplying by the lower graph and summing over r_3 and r_4, we obtain an expression which can be described using the labeling in Fig. 11(b). There is a $\sum_r$ for each internal vertex (i.e., r_3,r_4). There is a factor e^{ikr} for each decorated (predicted) arm in each EOM graph (i.e., for k_5, k_3', and k_4') and e^{-ikr} for each constrained one (k_3, k_4, k_1, and k_2). For each EOM graph there is a factor G [e.g., $G^{ee}_{ee}(k_3',k_4';k_1,k_2)$] and a factor such as $(2\pi)^d\delta_{2\pi}(k_3+k_4-k_1-k_2)$ expressing k-vector conservation. [In T-coarsening (Appendix A) we need not distinguish between G's in the L and S ensembles in the composite graphs, because the system is stationary.] There is a $\int dk/(2\pi)^d$ for each k vector; the integral can be taken over a d cube of side 2π located anywhere, because of the antiperiodicity of G. We can put together $\sum_r e^{ik'r-ikr}$ for each internal vertex (r_3 and r_4), and replace it by $(2\pi)^d\delta_{2\pi}(k'-k)$. This eliminates all the integrals over primed k's; we set $k'=k$ and do not need to put k labels on both sides of internal vertices. At this point we may change variables to single out the independent external k's (all but one will be independent) and the free internal k's; in this case these could be taken to be k_1, k_2, and an internal "momentum transfer" q, as shown in Fig. 11(c). We have chosen a variable h such that one of our δ functions is $\delta_{2\pi}(h)$; in general, we include such a variable for all but one of the EOM graphs. Our integrals are now over k_1, k_2, k_5, q, and h; that over h can be done using the δ function. In general, this leaves one δ function expressing overall conservation of k vector [in this case, $\delta_{2\pi}(k_5-k_1-k_2)$], in an expression which is exactly that defining the Fourier transform [Eq. (4.2) of Ref. 10]. The Fourier transform turns out to contain just the factors of G and the integrals over internal momenta.

Let us summarize the rules for evaluating a k-space ensemble-changing graph, for example, obtaining Eq. (2.11) [the Fourier-transform (FT) of Eq. (A4)] from the time-coarsening graph in Fig. 2.

(1) Label the lines in terms of the *independent* external and internal k vectors.

(2) Write a factor G for each constituent EOM graph, using the k's on the lines and the species labels α on the vertices.

(3) Write a d-dimensional integral $\int dk/(2\pi)^d$ for each internal k vector.

APPENDIX E: PERTURBATIVE CALCULATION OF EXPONENTIAL EOM'S

In this appendix we give a general procedure for calculating any propagator of an exponential EOM e^{E+F} as a power series in a perturbation generator F. By definition [Eq. (3.7)],

$$e^{E+F}=\lim_{du\to 0}\left[\prod_{du}(1+E\,du+F\,du)\right], \tag{E1}$$

where we have divided the time interval [0,1] into n intervals du. The product on the right-hand side (defined in Appendix B) can be expressed in terms of graphs (Appendix C); a particular propagator [call it $G'(e^{E+F})$] can be schematically written

$$G'(e^{E+F})=\sum_{\substack{\text{rosary}\\ \text{graphs}}}G_1(1+E\,du,F\,du)\times G_2(1+E\,du,F\,du)\cdots\ . \tag{E2}$$

A specific example in graphical form is the left-hand equality in Fig 3. The sum is over "rosary" graphs, such as the middle graph of Fig. 3, in which the system propagates successively through many small time intervals du. Each $G_i(1+E\,du,F\,du)$ is one of the propagators for such an interval; the notation means it can be a propagator of either of the EOM's $1_E+E\,du$ or $F\,du$. We single out those that involve the perturbation F and draw them explicitly in the rightmost graph [in Fig. 3 there is only one, the horizontal line $G^{\alpha\alpha}(k)$ at time u]. These F graphs break the collection of $1+E\,du$ graphs into connected components (two in Fig. 3); each component extends between two times u_{lower} and u_{upper}, each of which is 0, 1, or the time of an F graph. Such a component is exactly a graph in the expansion of a propagator of the unperturbed EOM $e^{E\,\Delta u}$, where $\Delta u=u_{\text{upper}}-u_{\text{lower}}$ (equal to $1-u$ in this case). We may collect the rosary graphs into classes which are topologically equivalent (i.e., are bounded by the same F graphs, perhaps at different times). We represent each such class by a "topological graph" such as the one on the right in Fig. 3. Each connected component is replaced by the corresponding propagator of the unperturbed EOM. The topological graph

will have the same numerical value as the sum of its rosary graphs if we sum over the times $u_1, u_2, \ldots$ of the F graphs.

The result of all this is the following set of rules for computing a propagator of a perturbed EOM e^{E+F}.

(1) Draw all possible topological graphs out of perturbation propagators (of the perturbing EOM F) at times $u_1, u_2, \ldots$ and unperturbed propagators extending between these times, according to the rules of Appendix D.

(2) For each graph, write the product of the unperturbed propagators (obtained from the EOM $e^{E\Delta u}$, where Δu is the difference of the relevant u's; in Eq. (3.9a) this is $\exp[-Dk^2(1-u)]$) and the perturbation propagators [ak^2 in Eq. (3.9)]. Integrate over internal wave vectors using the rules of Appendix D.

(3) Integrate over $u_1, u_2, \ldots$ subject to $0 < u_1 < u_2 < \cdots < 1$.

Applying these rules to Fig. 3 gives the fluctuation propagator at the fixed point [Eq. (3.9a)].

[1]S. Alexander, J. Bernasconi, W. R. Schneider, and R. Orbach, Rev. Mod. Phys. 53, 175 (1981).

[2]S. W. Haan and R. Zwanzig, J. Chem. Phys. 68, 1879 (1978).

[3]J. Klafter and S. Silbey, J. Chem. Phys. 72, 843 (1980).

[4]H. Scher and M. Lax, Phys. Rev. B 7, 4491 (1973).

[5]H. Scher and E. W. Montroll, Phys. Rev. B 12, 2455 (1975).

[6]J. Bernasconi, H. U. Beyeler, S. Strassler, and S. Alexander, Phys. Rev. Lett. 42, 819 (1979).

[7]R. Zwanzig, J. Stat. Phys. 28, 127 (1982).

[8]J. Machta, Phys. Rev. B 24, 5260 (1981).

[9]S. Alexander and R. Orbach, *Physica (Utrecht)* 107B, 675 (1981).

[10]P. B. Visscher, this issue preceding paper, Phys. Rev. B 29, 5462 (1984).

[11]P. B. Visscher, J. Stat. Phys. 25, 211 (1981).

[12]J. Kiefer and P. B. Visscher, in *Molecular-Based Study of Fluids,* Advances in Chemistry Series, edited by A. Mansoori and J. M. Haile (American Chemical Society, New York, 1983).

[13]Th. Niemeijer and J. M. J. van Leeuwen, in *Phase Transitions and Critical Phenomena,* edited by C. Domb and M. S. Green (Academic, New York, 1976), Vol. 6.

[14]See Ref. 10, Sec. VII.

[15]J. W. Haus, K. W. Kehr, and K. Kitahara, Z. Phys. B 50, 161 (1983).

[16]Equivalent results for two and three dimensions have also been recently obtained from a phenomenological fluctuating diffusion equation which gives expressions for the amplitudes related to the ones given here [M. H. Ernst, J. Machta, J. R. Dorfman, and H. van Beijeren, J. Stat. Phys. (to be published)].

[17]I. Webman and J. Klafter, Phys. Rev. B 26, 5950 (1982).

[18]J. W. Haus, K. W. Kehr, and K. Kitahara, Phys. Rev. B 25, 4918 (1982).

[19]P. J. H. Denteneer and M. H. Ernst, J. Phys. C (to be published).

[20]J. Kiefer and P. B. Visscher, J. Stat. Phys. 27, 389 (1982).

[21]M. Nelkin and A. K. Harrison, Phys. Rev. B 26, 6696 (1982).

[22]P. Grassberger and I. Procaccia, J. Chem. Phys. 77, 6281 (1982).

[23]P. B. Visscher, Physica 97A, 410 (1979).